Int. J. Heat Mass Transfer. Vol. 24, No. 7, pp. 1237–1245, 1981
Printed in Great Britain

0017–9310/81/071237–09 $02.00/0

HEAT TRANSFER ACROSS A VERTICAL IMPERMEABLE PARTITION IMBEDDED IN POROUS MEDIUM

ADRIAN BEJAN and REN ANDERSON
Department of Mechanical Engineering, University of Colorado, Boulder, CO 80309, U.S.A.

(*Received* 22 *September* 1980 *and in revised form* 6 *February* 1981)

Abstract — This article examines the buoyancy induced circulation occurring on both sides of a vertical impermeable partition separating two semi-infinite porous reservoirs maintained at different temperatures. The circulation is found to consist of two counterflowing boundary layers which interact thermally across the partition, transferring heat from the hot side to the cold side. The net heat transfer rate is calculated and the effect of the thickness and conductivity of the partition on the heat transfer rate is determined. It is demonstrated that the insertion of a vertical impermeable partition in the middle of a vertical porous layer reduces significantly the net heat transfer rate through the layer.

NOMENCLATURE

b, thermal stratification parameter;
C, constant of integration;
D, horizontal dimension of enclosure;
g, gravitational acceleration;
k, fluid-porous matrix conductivity;
k_w, wall conductivity;
K, permeability;
L, vertical dimension of partition;
Nu, Nusselt number;
Q, half temperature drop across wall;
Q_y, net heat transfer rate in the horizontal direction (per unit width);
Ra, Rayleigh number;
T^*, temperature;
T_c^*, cold side extreme temperature;
T_h^*, hot side extreme temperature;
T_0, wall temperature distribution;
W, wall thickness;
u^*, vertical velocity;
v^*, horizontal velocity;
x^*, vertical position;
y^*, horizontal position.

Greek symbols

α, thermal diffusivity;
β, coefficient of thermal expansion;
δ, horizontal length scale;
λ, boundary layer thickness, cold side;
ν, kinematic viscosity;
σ, boundary layer thickness, hot side;
ω, wall thermal resistance parameter.

Indices

c, cold side;
h, hot side;
–, average.

INTRODUCTION

IT IS known that the effectiveness of double walls filled with fibrous or granular insulating material is adversely affected by the natural circulation induced in the air which permeates through the insulation. The desire to conserve energy while heating buildings and refrigerating cold storage installations motivates an increasing amount of research into the fundamentals of buoyancy-induced heat transfer across spaces filled with air and a porous solid matrix.

The heat transfer across rectangular enclosures with different vertical wall temperatures and filled with fluid-saturated porous medium has been investigated by a number of authors (see, for example, [1–6]). A review of these studies shows that the heat leak through a vertical porous layer is reduced when the convective loop is slender (much taller than wide) [7]. In a vertical rectangular enclosure filled with porous material, the slenderness of the convective loop is dictated by the slenderness of the enclosure itself. One way of increasing the slenderness of the convection pattern is by inserting one or more vertical baffles (partitions) in the space filled with porous material. The baffles slice-off the original convective cell into a number of weaker and more slender vertical cells.

In connection with the engineering solution outlined above, we ask: how effective is a solid vertical partition in preventing the transfer of heat from one side to the other? The objective of the present article is to investigate the mechanism governing the transfer of heat across a solid impermeable wall vertically dividing a porous medium into two regions. To our knowledge, this mechanism has not been analyzed in the past. Therefore, we decided to study the phenomenon in its simplest and most fundamental configuration, namely, natural convection along the impermeable interface separating two semi-infinite por-

ous reservoirs maintained at different temperatures. In what follows we present an analytical solution for the boundary layer flow and temperature field around the impermeable partition. In the end, we use this solution to calculate the heat transfer rate across the arrangement and to evaluate the impact of partition properties (thickness, conductivity) and thermal stratification on the heat transfer rate.

MATHEMATICAL FORMULATION

Consider the two-dimensional configuration presented schematically in Fig. 1. A solid impermeable wall of height L and negligible thickness W separates two semi-infinite spaces filled with fluid-saturated porous medium. Far away from the wall the porous medium is considered isothermal, with a temperature T_h^* on the left (hot) side of the wall and a temperature T_c^* on the right (cold) side. In the cartesian system x–y, the dimensionless set of equations governing the conservation of mass, momentum and energy is

$$\frac{\partial u}{\partial x}+\frac{\partial v}{\partial y}=0 \tag{1}$$

$$\frac{\partial u}{\partial y}-\left(\frac{\delta}{L}\right)^2\frac{\partial v}{\partial x}=\frac{\partial T}{\partial y} \tag{2}$$

$$u\frac{\partial T}{\partial x}+v\frac{\partial T}{\partial y}=\left(\frac{\delta}{L}\right)^2\frac{\partial^2 T}{\partial x^2}+\frac{\partial^2 T}{\partial y^2} \tag{3}$$

where the dimensionless variables are defined as

$$x=x^*/L, \qquad y=y^*/\delta \tag{4),(5}$$

$$u=u^*\delta^2/(\alpha L), \qquad v=v^*\delta/\alpha \tag{6),(7}$$

$$T=\frac{T^*-\frac{1}{2}(T_h^*+T_c^*)}{T_h^*-T_c^*}. \tag{8}$$

In definitions (4)–(8) the asterisks indicate the dimensional variables of the problem. These variables are listed in the Nomenclature and on Fig. 1. On the basis of dimensional analysis one can show that the horizontal length scale δ is given by [3]

$$\delta=LRa^{-1/2} \tag{9}$$

where Ra is the Darcy-modified Rayleigh number based on L

$$Ra=\frac{g\beta KL}{\nu}(T_h^*-T_c^*). \tag{10}$$

It should be noted that the momentum equation was based as usual on the Darcy flow model and Boussinesq-incompressible fluid approximation. The porous medium is treated as homogeneous [8] where, for example, the thermal diffusivity ($\alpha=k/\rho c_p$) is based on the density and specific heat of the fluid and on the thermal conductivity k of the fluid-porous matrix combination.

We focus on the range of moderately high Rayleigh numbers so that, by equation (9), $\delta \ll L$. Consequently, in the following analysis we will neglect the terms containing $(\delta/L)^2$ in equations (2) and (3).

The temperature boundary conditions are

$$T\to -\tfrac{1}{2} \quad \text{as} \quad y\to\infty \tag{11}$$

$$T\to \tfrac{1}{2} \quad \text{as} \quad y\to -\infty \tag{12}$$

and, at the solid wall

$$T(x,0^-)=T(x,0^+) \tag{13}$$

$$\left(\frac{\partial T}{\partial y}\right)_{y=0^-}=\left(\frac{\partial T}{\partial y}\right)_{y=0^+}. \tag{14}$$

Conditions (13) and (14) recognize the fact that when the solid wall is thin (or of high conductivity) the temperature difference across the wall is negligible compared with the overall temperature difference. Also, the heat flux is conserved as it passes through the wall. The velocity boundary conditions are

$$u=0 \quad \text{as} \quad y\to\pm\infty \tag{15}$$

and, on both sides of the solid wall

$$v=0. \tag{16}$$

A discussion of the appropriate boundary conditions in the vertical direction, at $x+\pm\frac{1}{2}$, follows in the next section in which an analytical solution to equations (1)–(3) is developed based on the boundary layer approximation, $(\delta/L)\ll 1$.

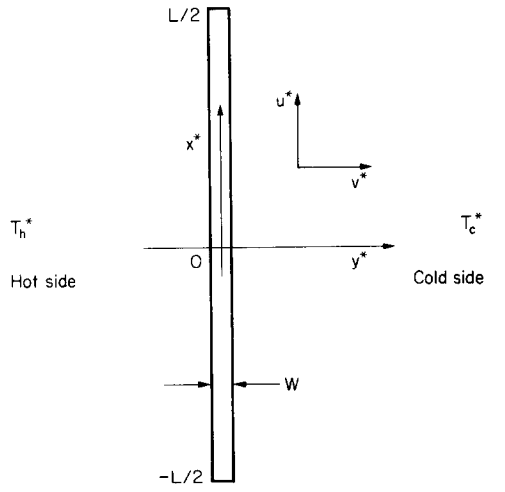

FIG. 1. Schematic of vertical impermeable partition imbedded in a fluid-saturated porous medium.

ANALYTICAL SOLUTION

An exact analytical solution to the above problem is not feasible due to the nonlinearity associated with the thermal convection terms in the energy equation (3). Although approximate, a powerful analytical approach consists of linearizing the energy equation in a way originally described by Ostrach [9] and Gill [10] in the context of buoyancy-induced convection. More recently, this method of solution was employed successfully in a number of studies dealing with free convection heat transfer in enclosures [3, 11, 12]. Of engineering importance is the fact that the overall heat

transfer results produced by these analyses agree extremely well with experimental and numerical heat transfer data [11, 12].

If we eliminate the temperature T between equations (2) and (3) we obtain

$$\frac{\partial^2 u}{\partial y^2} - (v)\frac{\partial u}{\partial y} - \left(\frac{\partial T}{\partial x}\right)u = 0. \tag{17}$$

The new energy equation (17) is linearized by regarding v and $\partial T/\partial x$ as unknown functions of x: $a(x)$ and $b(x)$. Based on these approximations equation (17) admits a solution of the form

$$u(x, y) = A_1 e^{r_1 y} + A_2 e^{r_2 y} \tag{18}$$

where $r_{1,2}$ are the roots of the characteristic equation

$$r^2 - a(x)r - b(x) = 0 \tag{19}$$

namely

$$r_{1,2} = a/2[1 \pm \sqrt{(1 + 4b/a^2)}]. \tag{20}$$

Function $b(x)$ represents the average vertical temperature gradient $\partial T/\partial x$ at fixed x in the boundary layer. Therefore, we expect $b(x)$ to be positive since on the right-hand side of the partition as the cold fluid rises it warms up gradually. Consequently, the two roots $r_1(x), r_2(x)$ are of opposite sign, regardless of the sign of $a(x)$. On the right (cold) side of the wall, the $y \to \infty$ velocity condition (15) is satisfied only if the positive root is discarded, i.e. if the corresponding coefficient A in equation (18) is set equal to zero. We conclude that the velocity solution for the cold side (subscript c) is of the form

$$u_c = A e^{-y/\lambda} \tag{21}$$

where, for reasons soon to become evident, we find it convenient to write $-1/\lambda$ in place of the negative root retained in the analysis. In expression (21), both A and λ are unknown functions of altitude x.

Substituting form (21) into the momentum equation (2) leads to the temperature distribution for the cold side

$$T_c = (T_0 + \tfrac{1}{2})e^{-y/\lambda} - \tfrac{1}{2} \tag{22}$$

which satisfies condition (11). In expression (22) $T_0(x)$ is the unknown temperature distribution along the partition. It is easy to show that with this notation the velocity distribution (21) can be rewritten as

$$u_c = (T_0 + \tfrac{1}{2})e^{-y/\lambda}. \tag{23}$$

A well-established property of free convection fields in systems differentially heated from side to side is the centrosymmetry [13] which, in Fig. 1, is about the point $x = 0$, $y = 0$. We rely on this property to immediately write for the hot side

$$T_h = (T_0 - \tfrac{1}{2})e^{y/\sigma} + \tfrac{1}{2} \tag{24}$$

$$u_h = (T_0 - \tfrac{1}{2})e^{y/\sigma} \tag{25}$$

without repeating the reasoning which led to expressions (22) and (23). Functions $\lambda(x)$ and $\sigma(x)$ are both positive and play the role of boundary layer thickness for the cold side and the hot side, respectively. Note that the centrosymmetry property requires

$$\sigma(x) = \lambda(-x). \tag{26}$$

The analytical solution (22)–(25) depends on three unknown functions, T_0, λ and σ. One relationship linking the three unknowns is the heat flux continuity statement (14), which yields

$$\frac{\lambda}{\sigma} = \frac{\frac{1}{2} + T_0}{\frac{1}{2} - T_0}. \tag{27}$$

We obtain two more equations by considering the integral form of the energy equation (3) for both sides of the partition

$$\frac{d}{dx}\int_0^\infty u_c T_c \, dy + |v_c T_c|_0^\infty = \left|\frac{\partial T_c}{\partial y}\right|_0^\infty \tag{28}$$

$$\frac{d}{dx}\int_{-\infty}^0 u_h T_h \, dy + |v_h T_h|_{-\infty}^0 = \left|\frac{\partial T_h}{\partial y}\right|_{-\infty}^0 \tag{29}$$

In these expressions v_c and v_h are the horizontal velocity distributions obtained from combining u_c and u_h with the mass conservation statement (1) and using the wall condition (16). Skipping a fair amount of algebra, the energy integrals (28) and (29) yield, respectively

$$\frac{d}{dx}\left[\frac{\lambda}{2}(\tfrac{1}{2} + T_0)^2\right] = \frac{1}{\lambda}(\tfrac{1}{2} + T_0) \tag{30}$$

$$\frac{d}{dx}\left[\frac{\sigma}{2}(\tfrac{1}{2} - T_0)^2\right] = -\frac{1}{\sigma}(\tfrac{1}{2} - T_0). \tag{31}$$

The solution for T_0, λ and σ is obtained by first evaluating σ based on equation (27) and substituting the result into equations (30) and (31). Next, the energy integrals (30) and (31) are added side by side, and the resulting equation is integrated once in x to yield

$$\lambda = C\frac{\frac{1}{2} + T_0}{\frac{1}{12} + T_0^2}. \tag{32}$$

Here, C is the constant of integration. Finally, we substitute equation (32) into the last form of the energy integral for the cold side and, after extensive manipulation, we find x as a function of T_0

$$\frac{2}{C^2}x = \int_0^{T_0} \frac{(\frac{1}{4} - m^2)^2}{(\frac{1}{12} + m^2)^3}\, dm \tag{33}$$

or, performing the integral

$$\frac{2}{C^2}x = 6\sqrt{3}\arctan(2\sqrt{3}\,T_0) + \frac{2T_0}{\frac{1}{12} + T_0^2} + \frac{T_0}{3(\frac{1}{12} + T_0^2)^2}. \tag{34}$$

The wall temperature $T_0(x)$ is, as required by centrosymmetry, an odd function of x [see equation (34)]. With $\lambda(x)$ given by equation (32) and $\sigma(x)$ given by equation (26), the analytical solution (22)–(25) is

now complete subject to the determination of constant C. The constant of integration must be determined from conditions applicable in the vertical direction, at $x = \pm\frac{1}{2}$. However, since the linearized solution (22)–(25) is of the boundary layer type, it can only be expected to hold in the central region of the wall sufficiently far from the ends [14]. Intentionally, we said little about the ends and nothing about the manner in which the wall separates the two porous media above $x = \frac{1}{2}$ and below $x = -\frac{1}{2}$.

Although under the present conditions there is no unique basis for determining constant C, we argue that when the partition is tall (Ra is high) the top end–bottom end temperature difference is asymptotically equal to the temperature difference between the hot side and the cold side. The reason for this becomes clear if we imagine the counterflow heat exchanger created by the boundary layer flow descending along the hot side and the stream rising along the cold side. The thermal contact between the two streams improves as the contact area (L) increases, to the point where the outlet temperature of one stream closely resembles the inlet temperature of the other. Since the two inlet temperatures are T_c^* and T_h^*, in the large L limit the wall temperature will also vary from T_c^* to T_h^*. Therefore, we used

$$T_0 = \pm\tfrac{1}{2} \quad \text{at} \quad x = \pm\tfrac{1}{2} \tag{35}$$

to evaluate the constant, and, from equation (34), we found $C = 0.255$.

RESULTS

The temperature of the vertical partition, equation (34), is shown plotted in Fig. 2. We see that T_0 varies almost linearly with x over roughly 80% of the height. At the top and bottom extremities where the solution breaks down, the wall temperature gradient dT_0/dx blows up.

The dimensionless boundary layer thickness $\lambda(x)$ is shown in Fig. 3; on the left-hand side of the figure we plotted $\sigma(x)$ which is the centrosymmetric of $\lambda(x)$

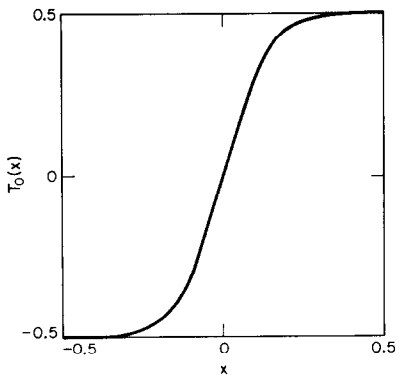

FIG. 2. Wall temperature distribution ($\omega = 0$).

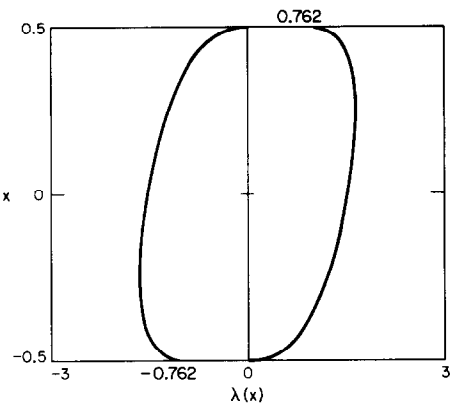

FIG. 3. Boundary layer thickness on the two sides of the partition ($\omega = 0$).

relative to the origin. The counterflowing boundary layers thicken up gradually in the direction of flow and terminate with finite values at the two exit points.

The temperature gradient in the horizontal direction, right at the wall, is shown in Fig. 4. The wall heat flux is practically uniform over most of the height and, at the two ends, it increases abruptly to finite values. Numerically, for the average wall heat flux we found

$$\overline{\left(-\frac{\partial T}{\partial y}\right)} = \int_{-1/2}^{1/2} \left(-\frac{\partial T}{\partial y}\right)_{y=0} dx = 0.382 \tag{36}$$

which is fairly close to the local heat flux at mid-height, $(-\partial T/\partial y)_{x=y=0} = 0.327$.

Representative streamlines and isotherms are illustrated in Figs. 5 and 6. The fluid motion is most intense near the wall where, thanks to the Darcy flow model, a non-slip condition cannot be imposed. The boundary layers entrain fluid from the lateral isothermal porous reservoirs. The isotherms of Fig. 6 show that the thermal interaction of the two porous media via the vertical partition is limited to the strip $-3 < y < 3$ which corresponds to a vertical slab no thicker than 6δ. In the central region of the wall the isotherms are almost parallel, verifying the conclusion reached earlier that the wall heat flux is almost uniform (see Fig. 4).

PARTITION WITH FINITE THERMAL RESISTANCE

In actual building insulation applications, the partition thickness W and conductivity k_w may have a noticeable effect on the net heat transfer rate between the two porous reservoirs. We determined this effect analytically by modifying the solution developed in the preceding sections.

If $2Q$ is the dimensionless temperature difference between the two faces of the partition, then the temperature and velocity distributions (22)–(25) attain the more general form

$$T_c = (T_0 - Q + \tfrac{1}{2})\exp\left[-\left(y - \frac{w}{2}\right)\Big/\lambda\right] - \tfrac{1}{2} \tag{37}$$

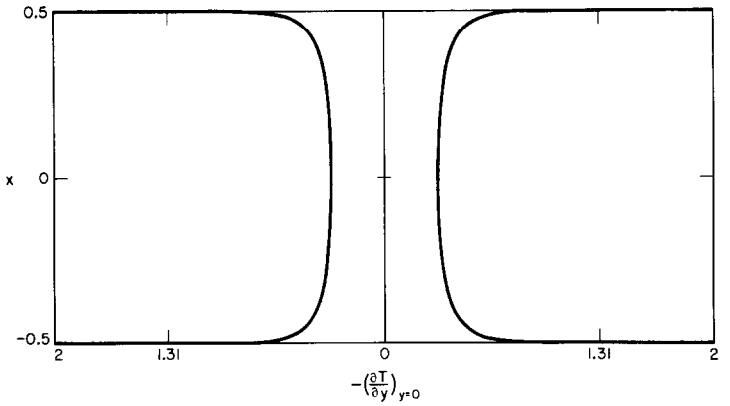

FIG. 4. Heat flux distribution along the partition ($\omega = 0$).

$$u_c = (T_0 - Q + \tfrac{1}{2})\exp\left[-\left(y - \frac{w}{2}\right)\Big/\lambda\right] \quad (38)$$

$$T_h = (T_0 + Q - \tfrac{1}{2})\exp\left[\left(y + \frac{w}{2}\right)\Big/\sigma\right] + \tfrac{1}{2} \quad (39)$$

$$u_h = (T_0 + Q - \tfrac{1}{2})\exp\left[\left(y + \frac{w}{2}\right)\Big/\sigma\right] \quad (40)$$

where

$$2Q = -w\left(\frac{\partial T}{\partial y}\right)_{y=\pm w/2} \quad (41)$$

$$w = W/\delta. \quad (42)$$

Note that Q is a function of vertical position along the partition. Equating the conduction heat flux through the wall with the convective flux at either surface ($y = \pm w/2$) we find

$$2Q = \omega(T_0 + \tfrac{1}{2})\Big/\left(\lambda + \frac{\omega}{2}\right) \quad (43)$$

where ω is the parameter describing the size of the wall thermal resistance relative to the convective (boundary layer) resistance

$$\omega = \frac{W}{L}\frac{k}{k_w}Ra^{1/2} \quad (44)$$

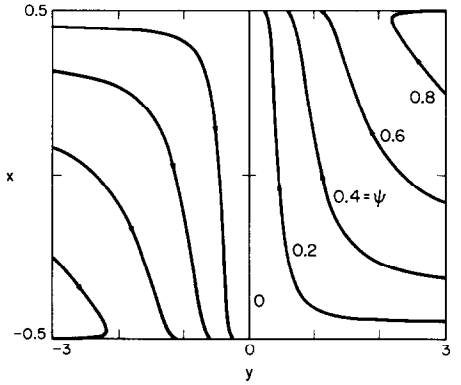

FIG. 5. Streamline pattern ($\omega = 0$).

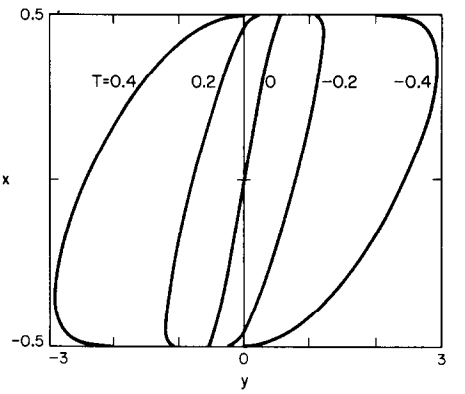

FIG. 6. Temperature distribution in the vicinity of the partition ($\omega = 0$).

Subjecting equations (37)–(40) to the analytical procedure which led to equation (32), we find

$$\frac{d}{dx}\left[\lambda(T_0 + \tfrac{1}{2})^2\Big/\left(1 + \frac{\omega}{2\lambda}\right)^2\right] = 2(T_0 + \tfrac{1}{2})\Big/\left(\lambda + \frac{\omega}{2}\right) \quad (45)$$

$$(T_0 + \tfrac{1}{2})^3 - \left(T_0 - \tfrac{1}{2} + \frac{\omega T_0}{\lambda}\right)^3 = \frac{3C}{\lambda}(T_0 + \tfrac{1}{2})\left(1 + \frac{\omega}{2\lambda}\right)^2. \quad (46)$$

Equation (45) results from applying the energy integral on the cold side of the partition. Equation (45) is analogous to (32) and results from integrating the sum of the two energy integrals with respect to x. Expressions (45) and (46) have already been simplified by eliminating Q based on equation (43).

Beyond this point the solution was carried out on a digital computer. We assumed again that in the two starting corners, ($x^* = L/2$, $y^* = -W/2$) and ($x^* = -L/2$, $y^* = W/2$) the surface temperature is equal to the porous reservoir temperature, T_h^* and T_c^*, respectively. Since T_0 is an odd function of x with $T_0(x = 0) = 0$, our numerical procedure began by guessing the value of C, calculating T_0 from equation (46) and

integrating equation (45) from $x = -\frac{1}{2}$ to $x = \frac{1}{2}$. The constant C was then readjusted and the whole procedure repeated until the hot starting corner temperature ($T_0 + Q$) coincided with $\frac{1}{2}$.

The results of the numerical solution are summarized in Table 1. Constant C decreases steadily as the wall thermal resistance parameter ω increases. We found $C(0) = 0.2547$, in close agreement with the earlier value $C = 0.255$ obtained analytically in the thin wall limit ($\omega = 0$).

The Nusselt number for overall heat transfer between the two reservoirs is shown in Table 1 and, graphically, in Fig. 7. The Nusselt number is defined as

$$Nu = \frac{Q_y}{k(T_h^* - T_c^*)} = \left(\overline{\frac{\partial T}{\partial y}}\right) Ra^{1/2} \tag{47}$$

where Q_y is the net heat exchange from T_h^* to T_c^*,

$$Q_y = kL\left(\overline{\frac{\partial T^*}{\partial y^*}}\right)_{y^* = \pm W/2}. \tag{48}$$

The coefficient in the $Nu \sim Ra^{1/2}$ proportionality (47) is shown in Table 1 and Fig. 7 as a function of ω. As expected, when the insulating capacity of the wall material (ω) increases, the net heat transfer rate (Nu) decreases. In the thermally thin wall limit the numerical solution yields $Nu = 0.3835Ra^{1/2}$ in good agreement with the analytical result $(\partial T/\partial y) = 0.382$, equation (36).

To illustrate the use of the $Nu(\omega, Ra)$ relationship presented in Fig. 7, consider a wooden partition ($W = 1$ cm, $L = 1$ m, $k_w = 2 \times 10^{-3}$ W cm^{-1} K^{-1}) mounted vertically inside a space (double wall) packed with glass wool ($k = 4 \times 10^{-4}$ W cm^{-1} K^{-1}). In such systems, the Rayleigh number based on wall height L is of the order of 10^3 or even higher [4]. Based on this information we calculate $\omega = 0.063$ and, consulting Table 1 and Fig. 7, we conclude that the heat transfer rate across the partition is 96% of the estimate based on the zero-thickness assumption ($\omega = 0$).

Table 1. Summary of numerical solution for wall with finite thermal resistance

ω	C	$(Nu/Ra^{1/2})^*$	$T_0(\frac{1}{2})$
0	0.2547	0.3835	0.5006
0.5	0.200	0.300	0.359
1	0.165	0.250	0.295
2	0.124	0.190	0.234
4	0.0859	0.129	0.174
6	0.066	0.0991	0.144
8	0.0537	0.0807	0.124
10	0.0457	0.0685	0.109

*Nusselt number correlation correct to within 1%; $Nu = 0.382(1 + 0.615\omega)^{-0.875} Ra^{1/2}$.

THE EFFECT OF THERMAL STRATIFICATION ON BOTH SIDES OF THE PARTITION

In order to assess the thermal insulation capability of a vertical partition imbedded in a porous space, it is important to recognize that the core region of such a space is thermally stratified (see Weber [3]). Therefore, we must determine the effect of thermal stratification on the heat transfer through the partition. Weber [3] showed that in a rectangular enclosure the vertical temperature gradient in the core is of order $\Delta T/L$, where ΔT is the temperature difference between the vertical walls. The temperature boundary conditions far away from the partition (11) and (12) are then

$$T \to \mp \tfrac{1}{2} + bx \quad \text{as} \quad y \to \pm \infty \tag{49}$$

where the dimensionless temperature gradient b is of order unity.

Following an analytical path identical to the one which led to the Oseen-linearized solution (22)–(25), we obtain

$$u_c = (T_0 + \tfrac{1}{2} - bx)e^{-y/\lambda} \tag{50}$$

$$T_c = (T_0 + \tfrac{1}{2} - bx)e^{-y/\lambda} - \tfrac{1}{2} + bx \tag{51}$$

$$u_h = (T_0 - \tfrac{1}{2} - bx)e^{y/\sigma} \tag{52}$$

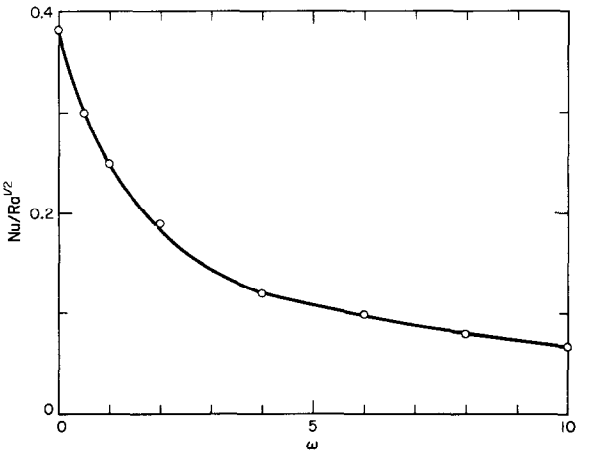

FIG. 7. Relationship between the net heat transfer rate and the thermal resistance of the partition.

$$T_h = (T_0 - \tfrac{1}{2} - bx)e^{y/\sigma} + \tfrac{1}{2} + bx. \quad (53)$$

The heat flux continuity condition (27) assumes the more general form

$$\frac{\lambda}{\sigma} = \frac{\frac{1}{2} - bx + T_0}{\frac{1}{2} + bx - T_0}. \quad (54)$$

Finally, the integral energy conditions (28) and (29) yield

$$\frac{d}{dx}\left[\frac{\lambda}{2}(T_0 + \tfrac{1}{2} - bx)^2\right] = \left(\frac{1}{\lambda} - b\lambda\right)(T_0 + \tfrac{1}{2} - bx) \quad (55)$$

$$\frac{d}{dx}\left[\frac{\sigma}{2}(T_0 - \tfrac{1}{2} - bx)^2\right] = \left(\frac{1}{\sigma} - b\sigma\right)(T_0 - \tfrac{1}{2} - bx). \quad (56)$$

The three unknown functions $T_0(x)$, $\lambda(x)$ and $\sigma(x)$ are determined from equations (54)–(56). However, unlike the $b = 0$ case [equations (27), (30) and (31)] which could be solved analytically, equations (54)–(56) require a numerical solution. We solved equations (54)–(56) on a digital computer by first expressing dT_0/dx, $d\lambda/dx$ and $d\sigma/dx$ as functions of (T_0, λ, σ). We integrated these expressions from $x = 0$ to $x = \frac{1}{2}$, taking $T_0(0) = 0$ and guessing the value of λ (or σ) at $x = 0$. At the end of the march, $x = \frac{1}{2}$, we sought to obtain $\sigma = 0$ (see the tip of the warm-side boundary layer, Fig. 3); if this condition was not satisfied, we adjusted the starting value of λ. This shooting procedure converges rapidly.

The main results of this numerical solution are presented in Table 2 and Fig. 8. As one might expect, the temperature gradient along the partition (T_0') increases as the stratification effect (b) becomes more pronounced. At the same time, the boundary layers become thinner and the heat transfer rate increases. In conclusion, the effect of thermal stratification is to accentuate the transfer of heat by natural convection through the vertical partition.

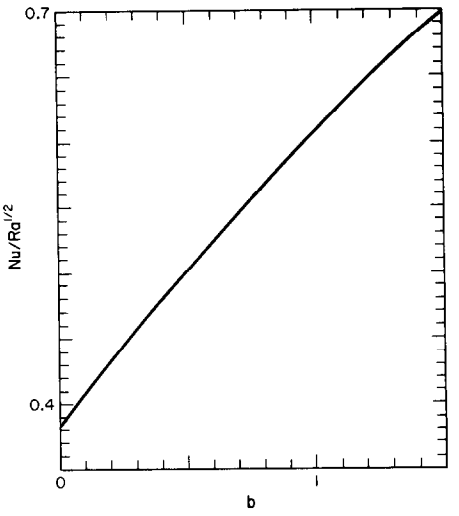

FIG. 8. Relationship between the heat transfer rate and the stratification on both sides of the partition.

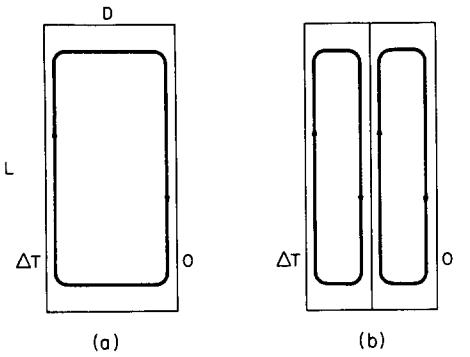

FIG. 9. Insulating porous layer (a) without and (b) with vertical impermeable partition.

INSULATION DESIGN CONSIDERATIONS

Returning to the engineering application which motivated this fundamental investigation, we are now in a position to assess the thermal insulation capability of a vertical partition imbedded in porous material. Consider the vertical rectangular enclosure (height L, thickness D) filled with porous insulation shown in Fig. 9. The vertical faces of the enclosure are at different temperatures, 0 and ΔT. If natural convection is the dominant mode of heat transfer across the porous layer, then Weber's result [3] can be used to calculate the horizontal heat transfer rate

$$Q_y = 0.577k\Delta TRa^{1/2}. \quad (57)$$

Here Ra is based on L and ΔT, therefore the wall-to-wall heat transfer rate is independent of the wall-to-wall spacing D. The heat transfer is effected by a clockwise convective loop, the boundary layer thickness being considerably smaller than D. The inner region sandwiched between the two boundary layers contains nearly stagnant fluid.

Consider now the insulation effect of one partition, as shown on the right-hand side of Fig. 9. Symmetry suggests that the temperature in the center of the partition is $\Delta T/2$. Also, the midheight temperatures in the two core regions are, approximately, $3\Delta T/4$ and $\Delta T/4$. Furthermore, the core stratification is such that

Table 2. Summary of numerical results for the effect of thermal stratification (b) on the heat transfer rate through the partition

b	$\lambda_{x=0}$	$(T_0')_{x=0}$	$Nu/Ra^{1/2}$
0	1.530	0.285	0.382
0.25	1.323	0.464	0.444
0.5	1.168	0.655	0.501
0.75	1.045	0.860	0.556
1	0.948	1.075	0.606
1.25	0.868	1.301	0.655
1.5	0.803	1.534	0.699

the top of the left core has a temperature of order ΔT, while the bottom of the right core has a temperature of order 0 (Weber [3]). Therefore the partition is exposed to a midheight temperature difference of order $\delta T = \Delta T/2$, while the stratification parameter b is of order unity on both sides of the partition. The heat transfer rate through the partition is (from Fig. 8, $b = 1$)

$$Q_y \cong 0.606k\delta TRa_{\delta T}^{1/2} \quad (58)$$

or, in terms of the overall temperature difference $\Delta T = 2\delta T$

$$Q_y \cong 0.214k\Delta TRa^{1/2}. \quad (59)$$

Comparing equations (59) and (57) we conclude that the insertion of one partition through the middle of an insulation-packed double wall has the effect of reducing the heat transfer rate by approximately 63%. From an engineering standpoint this is a sizeable reduction, especially when we recognize that the design change from Fig. 9(a) to Fig. 9(b) does not affect the overall dimensions of the insulation system.

CONCLUSIONS

In order to calculate the insulating effect of a vertical partition imbedded in a double wall filled with porous material, we first analyzed the more fundamental phenomenon of natural convection about an impermeable wall separating two semi-infinite porous reservoirs at different temperatures. In the first part of this article we demonstrated that the net heat transfer between reservoirs across the partition is effected via two counterflow boundary layers lining the two faces of the partition. We were able to determine the heat transfer rate as well as the relation between it and partition properties (thickness and conductivity) and the degree of thermal stratification on both sides of the partition. We concluded the article by showing that the insertion of one vertical partition in the middle of a vertical porous layer drastically reduces the net heat transfer through the layer. The corresponding insulation effect associated with a vertical partition separating fluids at different temperatures was studied by Anderson and Bejan [15].

Acknowledgement — This research was supported by the National Science Foundation through grant no. ENG. 78-20957.

REFERENCES

1. B. K. C. Chan, C. M. Ivey and J. M. Barry, Natural convection in enclosed porous media with rectangular boundaries, *J. Heat Transfer* **92,** 21 (1970).
2. C. G. Bankvall, Natural convection in vertical permeable space, *Warme- und Stoffübertragung* **7,** 22 (1974).
3. J. E. Weber, The boundary-layer regime for convection in a vertical porous layer, *Int. J. Heat Mass Transfer* **18,** 569 (1975).
4. P. J. Burns, L. C. Chow and C. L. Tien, Convection in a vertical slot filled with porous insulation, *Int. J. Heat Mass Transfer* **20,** 919 (1977).
5. A. Bejan and C. L. Tien, Natural convection in a horizontal porous medium subjected to an end-to-end temperature difference, *J. Heat Transfer* **100,** 191 (1978).
6. K. L. Walker and G. M. Homsy, Convection in a porous cavity, *J. Fluid Mech.* **87,** 449 (1978).
7. A. Bejan, A synthesis of analytical results for natural convection heat transfer across rectangular enclosures, *Int. J. Heat Mass Transfer* **23,** 723 (1980).
8. J. W. Elder, Steady free convection in a porous medium heated from below, *J. Fluid Mech.* **27,** 29 (1966).
9. S. Ostrach, Natural convection in enclosures, *Adv. Heat Transfer* **8,** 161 (1972).
10. A. E. Gill, The boundary-layer regime for convection in a rectangular cavity, *J. Fluid Mech.* **26,** 515 (1966).
11. A. Bejan, Note on Gill's solution for free convection in a vertical enclosure, *J. Fluid Mech.* **90,** 561 (1979).
12. A. Bejan, On the boundary layer regime in a vertical enclosure filled with a porous medium, *Lett. Heat Mass Transfer* **6,** 93 (1979).
13. D. E. Cormack, L. G. Leal and J. H. Seinfeld, Natural convection in a shallow cavity with differentially heated end walls. Part 2. Numerical solutions, *J. Fluid Mech.* **65,** 231 (1974).
14. C. Quon, Free convection in an enclosure revisited, *J. Heat Transfer* **99,** 340 (1977).
15. R. Anderson and A. Bejan, Natural convection on both sides of a vertical wall separating fluids at different temperatures, *J. Heat Transfer* **102,** 630 (1980).

TRANSFERT THERMIQUE A TRAVERS UNE PARTITION VERTICALE IMPERMEABLE NOYEE DANS UN MILIEU POREUX

Résumé—On examine la circulation naturelle induite au voisinage des deux faces d'une cloison verticale, imperméable qui sépare deux réservoirs poreux semi-infinis, maintenus à des températures différentes. La circulation consiste en deux couches limites à contre-courant qui interagissent thermiquement à travers la cloison pour transférer la chaleur du côté chaud vers le côté froid. Le flux thermique net transféré est calculé et l'effet de l'épaisseur et de la conductivité de la cloison sur le transfert est déterminé. On démontre que l'insertion d'une cloison verticale au milieu d'une couche poreuse verticale réduit sensiblement le flux thermique à travers la couche.

WÄRMETRANSPORT DURCH EINE IN PORÖSEM MEDIUM EINGEBETTETE VERTIKALE UNDURCHLÄSSIGE TRENNWAND

Zusammenfassung—Der Bericht behandelt die durch Auftrieb induzierte Zirkulation, die auf beiden Seiten einer vertikalen undurchlässigen Trennwand auftritt, welche zwei auf unterschiedlichen Temperaturen gehaltene halbunendliche poröse Reservoire trennt. Es wird festgestellt, daß die Zirkulation aus zwei entgegengesetzt strömenden Grenzschichten besteht, die sich durch die Trennwand hindurch thermisch beeinflussen und Wärme von der warmen zur kalten Seite übertragen. Es wird der Gesamtwärmeübergang. berechnet und der Einfluß der Dicke und Wärmeleitfähigkeit der Trennwand auf den Wärmeübergang bestimmt. Es wird gezeigt, daß das Einfügen einer vertikalen undurchlässigen Trennwand in der Mitte einer vertikalen porösen Schicht den Gesamtwärmedurchgang durch die Schicht wesentlich reduziert.

ТЕПЛОПЕРЕНОС ЧЕРЕЗ ВЕРТИКАЛЬНУЮ НЕПРОНИЦАЕМУЮ ПЕРЕГОРОДКУ, ПОМЕЩЕННУЮ В ПОРИСТУЮ СРЕДУ

Аннотация — Исследуется вызванная силами выталкивания циркуляция на обеих поверхностях вертикальной непроницаемой перегородки, разделяющей два полубесконечных пористых резервуара, находящихся при разных температурах. Найдено, что циркулирующий поток состоит из двух движущихся в противоположных направлениях пограничных слоев, между которыми происходит тепловое взаимодействие через перегородку, передающую тепло от нагретого резервуара к холодному. Дан расчет суммарной интенсивности переноса тепла и определено влияние толщины и теплопроводности перегородки на интенсивность теплопереноса. Показано, что вертикальная непроницаемая перегородка, помещенная по середине вертикального пористого слоя, значительно снижает суммарную интенсивность переноса тепла через слой.